Kinetics of Acetyl Radical Formation from Methyl Radicals and Carbon Monoxide and Crystal Structures of Two Acetylcobalt Complexes

Andreja Bakac,* James H. Espenson, and Victor G. Young, Jr.

Ames Laboratory and Department of Chemistry, Iowa State University, Ames, Iowa 50011

Received August 21, 1992

Methyl radicals react with macrocyclic cobalt complexes $(H_2O)_2LCo^{2+}$ (L^1 = 1,4,8,11-tetraazacyclotetradecane, L^2 = *C-meso*-5,7,7,12,14,14-hexamethyl-1,4,8,11-tetraazacyclotetradecane) in the presence of CO in acidic aqueous solution. The reaction yields a mixture of methyl and acetyl complexes as a result of the competition between CO and $(H_2O)_2CoL^{2+}$ for $CH_3^\bullet$. Kinetic competition experiments yielded the rate constant for the capture of $CH_3^\bullet$ by CO, $k_{CO} = (2.0 \pm 0.3) \times 10^6$ M^{-1} s^{-1}. The acetyl complex of CoL^1 crystallizes with either H_2O or ClO_4^- coordinated trans to the acetyl group. Both the red $[(ClO_4)L^1CoC(O)CH_3](ClO_4)$ (**1**) and the yellow $[(H_2O)L^1CoC(O)CH_3](ClO_4)_2 \cdot H_2O$ (**2**) crystallize in the centric space group $P2_1/c$ with four molecules in a unit cell of dimensions $a = 10.539$ (1) Å, $b = 12.548$ (2) Å, $c = 14.915$ (2) Å, and $\beta = 93.74$ (3)° for **1** and $a = 12.588$ (3) Å, $b = 8.821$ (3) Å, $c = 19.398$ (5) Å, and $\beta = 96.34$ (2)° for **2**. The data refined to final values of the unweighted *R* factors of 0.037 (**1**) and 0.054 (**2**).

Introduction

The formation of carbon–carbon bonds is one of the major goals of synthetic organic and organometallic chemistry. The reaction of alkyl radicals with carbon monoxide (eq 1) has not been given much attention in that context, even though this reaction is thermodynamically favorable for some radicals. The reason for the apparent lack of interest in reaction 1 is probably the (presumed) low value of the rate constant k_1 and the low solubility of CO in common solvents. Both of these factors would tend to diminish the rate of formation and the yield of the acyl radicals and lead to the loss of alkyl radicals in the rapid self-reactions of eq 2 at atmospheric pressures of CO.

$$R^\bullet + CO \rightleftarrows RC^\bullet O \quad k_1, k_{-1} \tag{1}$$

$$2R^\bullet \rightarrow \{R_2 + RH + R(-H)\} \tag{2}$$

A kinetic study[1] of the gas-phase reaction of methyl radicals with CO (eq 3) yielded the rate constants $k_{CO} = 6.5 \times 10^3$ M^{-1} s^{-1} and $k_{-CO} = 7.3$ s^{-1} at 25 °C. One might have expected[2] that

$$CH_3^\bullet + CO \rightleftarrows CH_3C^\bullet O \quad k_{CO}, k_{-CO} \tag{3}$$

the rate constants in solution would be similar to those in the gase phase, but the synthetic success[3a] of a Fenton-type reaction involving CO and organic substrates seems to argue against it. Specifically, if reaction 1 is indeed involved in the reported[3a] preparation of carboxylic acids, then it must be much faster than reaction 2 in aqueous solution at room temperature and atmospheric pressure for the radicals derived from alcohols, amines, nitriles, and acids. This is striking, since the steady-state concentrations of the radicals had to be large under the experimental conditions[3a] and all the radicals involved should add CO more slowly than $CH_3^\bullet$ does. This result requires that the rate constant for the reaction with $CH_3^\bullet$, k_3, be much greater in solution than the reported gas-phase value.[1] A recent report[3b] on free radical carbonylations in benzene under moderate CO pressures also indicates that the capture of CO by alkyl radicals is faster than previously thought.

The apparent discrepancy between the gas-phase kinetic data[1] and solution-phase chemistry[3] has prompted us to examine reaction 3 in aqueous solution. We were specifically interested in finding out whether reactions 1 and 3 can be useful as a synthetic route to acyl radicals at atmospheric pressures. Our preliminary findings have been published.[4] In addition we sought to learn whether the hydration reaction interconverting to $CH_3C^\bullet O$ and $CH_3C^\bullet(OH)_2$ plays a role. We have been able to show that photohomolysis of the acetyl cobalt complexes leads only to $CH_3C^\bullet O$. Subsequent hydration then yields $CH_3C^\bullet(OH)_2$.

Complexes of two macrocyclic ligands were used, L^1 = [14]aneN$_4$ = 1,4,8,11-tetraazacyclotetradecane and L^2 = Me_6[14]aneN$_4$ = *C-meso*-5,7,7,12,14,14-hexamethyl-1,4,8,11-tetraazacyclotetradecane.

Experimental Section

Preparation of $[L^1CoC(O)CH_3](ClO_4)_2$. A CO-saturated solution of 0.47 g of $[(H_2O)L^1CoCH_3](ClO_4)_2$[5] in 800 mL of 0.05 M $HClO_4$ in a Pyrex Erlenmeyer flask was photolyzed at ~5 °C for 2 h with a 300-W sun lamp. The bubbling with CO was continued throughout the photolysis. After the color changed from a pale orange-yellow to an intense bright yellow, the complex was loaded on a column of SP Sephadex C-25 cation-exchange resin, rinsed with 0.1 M $HClO_4$, and then eluted with 1.0 M $HClO_4$. Slow evaporation in a hood yielded a precipitate which was filtered off, washed with a minimum amount of ice-cold water, and dried in a vacuum desiccator. Yield: 0.3 g (64%). Cobalt analysis: found, 11.9%; calculated, 11.8% for $[(ClO_4)L^1CoC(O)CH_3](ClO_4)$ (**1**) and 11.4% for $[(H_2O)L^1CoC(O)CH_3](ClO_4)_2 \cdot H_2O$ (**2**). Both forms yield the same solution species, which we presume to be $(H_2O)L^1CoC(O)CH_3^{2+}$.

The same procedure was used to prepare $[(H_2O)L^2CoC(O)CH_3](ClO_4)_2$ from $[(H_2O)L^2CoCH_3](ClO_4)_2$, except that the ion-exchange step had to be done under argon to prevent air oxidation of the complex.

The cobalt(II) complex $[L^2Co(H_2O)_2](CF_3SO_3)_2$ was prepared as previously reported.[6] $L^1Co(H_2O)_2^{2+}$ was prepared in solution[5] and used within 2 h of preparation.

(1) Watkins, K. W.; Word, W. W. *Int. J. Chem. Kinet.* **1974**, *6*, 855.
(2) Goldberg, K. I.; Bergman, R. G. *J. Am. Chem. Soc.* **1989**, *111*, 1285.
(3) (a) Coffman, D. D.; Cramer, R.; Mochel, W. E. *J. Am. Chem. Soc.* **1958**, *80*, 2882. (b) Ryu, I.; Kusano, K.; Ogawa, A.; Kambe, N.; Sonoda, N. *J. Am. Chem. Soc.* **1990**, *112*, 1295.
(4) (a) Bakac, A.; Espenson, J. H. *J. Chem. Soc., Chem. Commun.* **1991**, 1497. (b) Bakac, A.; Espenson, J. H. *Abstracts of Papers*, 203rd National Meeting of the American Chemical Society, San Francisco, CA; American Chemical Society: Washington, DC, 1992; INOR 809. The abstract states erroneously that complex **1** crystallizes in a pentacoordinated form.
(5) Bakac, A.; Espenson, J. H. *Inorg. Chem.* **1987**, *26*, 4353.
(6) Bakac, A.; Espenson, J. H. *Inorg. Chem.* **1990**, *29*, 2062.

0020-1669/92/1331-4959$03.00/0

Table I. Crystal Data for $[(ClO_4)L^1CoC(O)CH_3](ClO_4)$ and $[(H_2O)L^1CoC(O)CH_3](ClO_4)_2 \cdot H_2O$

formula	$[CoN_4C_{12}H_{27}O](ClO_4)_2$	$[CoN_4C_{12}H_{29}O_2](ClO_4)_2 \cdot H_2O$
fw	501.21	537.23
space group	$P2_1/c$	$P2_1/c$
a, Å	10.539 (1)	12.588 (3)
b, Å	12.548 (2)	8.821 (3)
c, Å	14.915 (2)	19.398 (5)
β, deg	93.74 (3)	96.34 (2)
V, Å^3	1968 (1)	2138 (1)
Z	4	4
d_{calc}, g/cm^3	1.69	1.67
cryst size, mm	0.40 × 0.30 × 0.20	0.40 × 0.40 × 0.35
radiation	MoKα (λ = 0.710 73 Å)	CuKα (λ = 1.541 78 Å)
data collection instrument	Enraf-Nonius CAD-4	Siemens P4RA
μ, cm^{-1}	12.3	91.7
temp, K	293	193
scan method	θ–2θ	θ–2θ
data collection range, deg	4.0–55.0	4–115
no. of data collected	9507	7024
no. of unique data with $F_o^2 > 3.0\sigma(F_o)^2$	4722	2873
R_{int}	0.016	0.042
no. of params refined	280	299
transm factors: max, min (ψ-scans)	0.999, 0.903	0.5396, 0.2877
R^a	0.037	0.054
R_w^b	0.055	0.062
quality of fit indicator^c	1.53	2.22
largest shift/esd, final cycle	0.00	0.06
largest peak, e/Å^3	0.70 (4)	0.52

$^a R = \sum||F_o| - |F_c||/\sum|F_o|$. $^b R_w = [\sum w(|F_o| - |F_c|)^2/\sum w|F_o|^2]^{1/2}$; $w = 1/\sigma^2(|F_o|)$. ^{c} Quality of fit $= [\sum w(|F_o| - |F_c|)^2/(N_{observns} - N_{params})]^{1/2}$.

Warning. Perchlorate salts of transition metal complexes, especially those containing [14]aneN$_4$ and related ligands, are potentially explosive. Special care must be taken in preparation and handling of such complexes.

Crystallographic Analysis of 1. Crystals suitable for diffraction analysis were obtained by slow evaporation of a 0.01 M $HClO_4$ solution of $(H_2O)L^1CoC(O)CH_3^{2+}$ in a refrigerator over a period of several weeks. A dark red crystal of **1** was mounted on a glass fiber for crystallographic analysis on an Enraf-Nonius CAD4 automated diffractometer at 20 °C. The unit cell was determined and refined from 25 randomly selected reflections obtained by employing the CAD4 automatic search, center, index, and least-squares routines.[7] Pertinent crystal and data collection parameters for **1** are presented in Table I. Data processing was performed on a MicroVax II computer using the SDP programs. The data were corrected for decay on the basis of a set of standard reflections which were repeated hourly and for absorption on the basis of on a series of ψ-scans by means of the empirical absorption method. Neutral-atom scattering factors were calculated and anomalous dispersion corrections were applied to all atoms. The space group $P2_1/c$ was established by the systematic absences. The structure was determined by direct methods using SHELX-86.[8]

Anisotropic refinement of all non-hydrogen atoms and analysis of subsequent difference-Fourier map revealed positions of all hydrogen atoms. The acetyl hydrogens were placed directly from the difference-Fourier map, while the remainder were ideally placed using C–H and N–H bond distances of 0.95 and 0.89 Å, respectively. All hydrogens were refined with isotropic temperature factors. Selected bond lengths, angles, and torsion angles are presented in Table II.

Crystallographic Analysis of 2. Crystals suitable for structure determination were grown from an aqueous solution of $(H_2O)L^1CoC(O)CH_3^{2+}$ in dilute $HClO_4/NaClO_4$ over a period of 1–2 months. A yellow crystal of **2** was mounted on a glass fiber for crystallographic analysis using a Siemens P4RA diffractometer at −80 °C. The unit cell was determined from 20 reflections taken from a rotation photograph. Axial photographs indicated the presence of a monoclinic lattice. The reflections were initially found, centered, and refined using the Siemens P3 software. All crystallographic calculations were accomplished with the SHELXTL-Plus programs[9] on a VaxStation 3100 computer. The pertinent crystal and data collection parameters for **2** are presented in Table I. A correction for decay based on a series of standard reflections was applied to the data. Similarly, a correction was applied for absorption based on several azimuthal scans using the semiempirical methods. The structure was solved using direct methods.[10]

All non-hydrogen atoms were refined anisotropically. The subsequent analysis of difference-Fourier maps led to positions for all hydrogen atoms except for the water of crystallization.

Kinetic competition experiments for the determination of k_3 were carried out with CO-saturated solutions containing variable amounts of $LCo(H_2O)_2^{2+}$ and *t*-BuOOH. After the completion of the reaction, a small excess of Cr^{2+} was added to reduce the strongly light-absorbing $LCo(H_2O)_2^{3+}$ to the weakly absorbing 2+ ion. The yields of $(H_2O)LCoC(O)CH_3^{2+}$ were determined spectrophotometrically with due allowance for the contribution to the absorbance by $LCo(H_2O)_2^{2+}$ and $(H_2O)LCoCH_3^{2+}$; see Table II.

Table II. UV–Visible Spectral Data for $(H_2O)LCoR^{2+}$ Complexes[a]

L	R	λ_{max}, nm (ϵ M^{-1} cm^{-1})	source
L^1	CH_3	476 (81), 368 (106)	ref 5
L^2	CH_3	500 (72.4), 384 (117)	*b*
L^1	$C(O)CH_3$	452 (90.8), 319 (1190)	this work
L^2	$C(O)CH_3$	472 (81), 324 (834)	this work
L^1	H_2O	465 (21.5), 320 (10)	*c*
L^2	H_2O	482 (70), 332 (43.8)	*b*

[a] In 0.01 M aqueous $HClO_4$. L^1 = [14]aneN$_4$; L^2 = Me$_6$[14]aneN$_4$. [b] Bakac, A.; Espenson, J. H. *J. Am. Chem. Soc.* **1990**, *112*, 2273. [c] Reference 18b. Due to a typographical error, this reference reported the position of the first maximum as 560 nm.

Table III. Selected Bond Lengths (Å), Bond Angles (deg), and Torsional Angles (deg) for **1** and **2**[a]

	1	**2**	
	Bond Lengths		
Co–N(1)	1.981 (2)	1.971 (4)	
Co–N(2)	1.986 (2)	1.990 (4)	
Co–N(3)	1.972 (2)	1.988 (5)	
Co–N(4)	1.973 (2)	1.970 (4)	
Co–C(11)	1.929 (2)	1.911 (6)	
Co–O*	2.320 (2)	2.207 (4)	
C(11)–O(1)	1.205 (3)	1.233 (7)	
C(11)–C(12)	1.507 (4)	1.47 (1)	
	Bond Angles		
Co–C(11)–C(12)	122.6 (2)	124.1 (4)	
Co–C(11)–O*(1)	118.0 (2)	119.7 (5)	
N(1)–Co–N(2)	85.3 (1)	85.7 (2)	
N(1)–Co–N(3)	172.29 (9)	174.8 (2)	
N(1)–Co–N(4)	90.47 (9)	93.3 (2)	
N(2)–Co–N(3)	96.6 (1)	94.6 (2)	
N(2)–Co–N(4)	170.49 (9)	175.1 (2)	
N(3)–Co–N(4)	86.6 (1)	85.9 (2)	
N(1)–Co–C(11)	93.7 (1)	93.4 (2)	
N(2)–Co–C(11)	89.7 (1)	90.9 (2)	
N(3)–Co–C(11)	93.8 (1)	91.8 (2)	
N(4)–Co–C(11)	99.1 (1)	93.9 (2)	
N(1)–Co–O*	89.01 (8)	84.6 (2)	
N(2)–Co–O*	83.60 (8)	88.7 (2)	
N(3)–Co–O*	83.77 (8)	90.2 (2)	
N(4)–Co–O*	87.82 (8)	86.4 (2)	
	Torsional Angles		
N(1)–Co–C(11)–O	−48.7 (3)	45.1 (5)	93.8
N(2)–Co–C(11)–O	36.5 (3)	130.9 (5)	94.4
N(3)–Co–C(11)–O	133.1 (3)	−134.5 (5)	92.4
N(4)–Co–C(11)–O	−139.8 (3)	−48.5 (6)	91.3
			93.0

[a] O*: in **1**, O–ClO_3^-, and in **2**, OH_2.

(7) *Enraf-Nonius Structure Determination Package*; Enraf-Nonius: Delft, Holland. Neutral-atom scattering factors and anomalous scattering corrections were taken from: *International Tables for X-ray Crystallography*; The Kynoch Press: Birmingham, England, 1974; Vol. IV.
(8) Sheldrick, G. M. SHELXS-86. Institut fur Anorganische Chemie der Universitat Gottingen, Germany.
(9) R3 m/V Crystallographic Software, Siemens Analytical X-ray Instruments, Inc., Madison, WI.
(10) SHELXTL Plus, Siemens Analytical X-ray Instruments, Inc., Madison, WI.

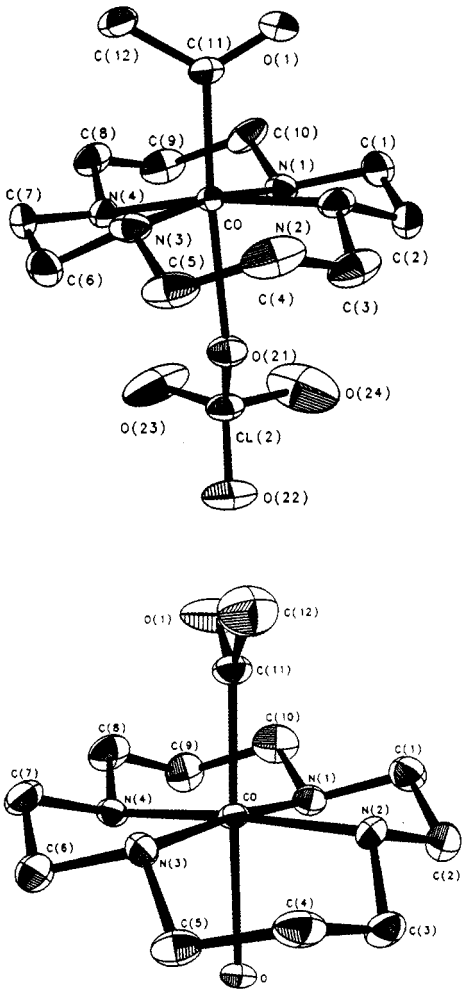

Figure 1. ORTEP diagrams of $[(ClO_4)L^1CoC(O)CH_3](ClO_4)$ (**1**) and $[(H_2O)L^1CoC(O)CH_3](ClO_4)_2 \cdot H_2O$ (**2**). L^1 = [14]aneN$_4$.

All the UV–visible spectral and some kinetic data were collected by use of Cary 219, Perkin-Elmer Lambda Array 3840, and Shimadzu UV 3101 PC spectrophotometers. ^1H and ^{13}C NMR spectra were recorded by use of a Varian XM 300 spectrometer. The IR spectra were obtained by use of a Perkin-Elmer FTIR 1800 instrument equipped with a Model 200 MTEC photoacoustic detector.

The kinetics of the oxidation of the hydrated acetyl radical, $CH_3{}^{\bullet}C(OH)_2$, by $C(NO_2)_4$ were measured by the dye laser flash photolysis system described earlier.[11] The excitation wavelength was 490 nm (Exciton LD 490 dye), and the progress of the reaction was monitored at 350 nm. The kinetics of the reaction of Cr^{2+} with $CH_3C^{\bullet}O$ were determined by use of an Applied Photophysics NdYAG laser system. The excitation wavelength of 355 nm and a monitoring wavelength of 320 nm were used. The reactions of $(CH_3)_3COOH$ with $LCo(H_2O)_2^{2+}$ complexes (L = L^1 and L^2) were monitored by conventional spectrophotometry at 320 nm under pseudo-first-order conditions with the cobalt(II) complexes (0.3–2 mM) in excess over the peroxide (0.04–0.1 mM).

All the kinetic data were obtained under strictly anaerobic conditions (Ar or CO).

Results

X-ray crystal structures of $[(ClO_4)L^1CoC(O)CH_3](ClO_4)$ (1) and $[(H_2O)L^1CoC(O)CH_3](ClO_4)_2 \cdot H_2O$ (2) are represented by the ORTEP drawings in Figure 1. The crystallographic data for both are summarized in Table I. Selected bond distances and bond angles are given in Table III. Complete listings of positional parameters, thermal parameters, bond distances, and bond angles and unit cell packing diagrams are given in the supplementary material. The bond distances and bond angles within the macrocycle for both acetyl complexes are almost identical with those in the ethyl complex, $[(H_2O)L^1CoCH_2CH_3](ClO_4)_2$.[5]

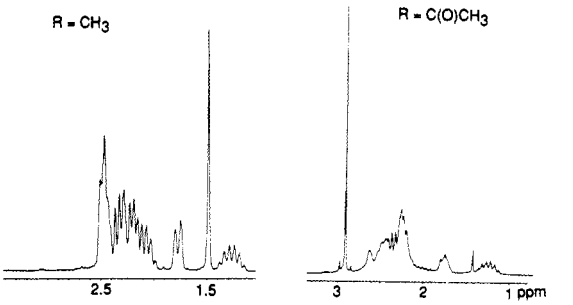

Figure 2. ^1H NMR spectra of $L^1CoCH_3^{2+}$ and $L^1CoC(O)CH_3^{2+}$ in D_2O (L^1 = [14]aneN$_4$). The methyl groups appear as sharp singlets at 1.48 and 2.91 ppm, respectively.

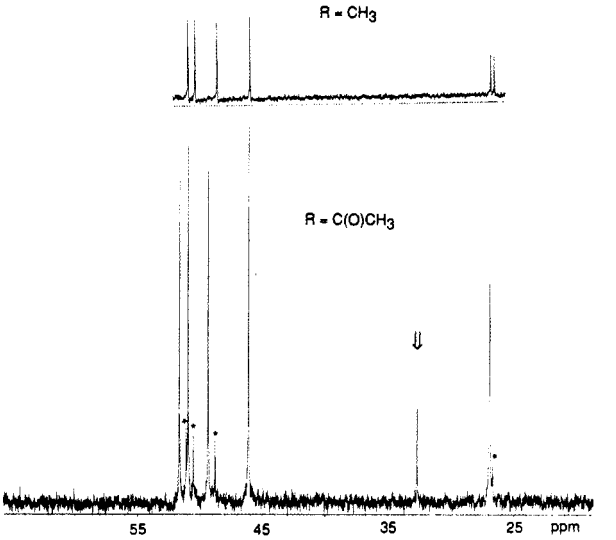

Figure 3. ^{13}C NMR spectrum of $(H_2O)L^1CoC(O)CH_3^{2+}$ in D_2O (L^1 = [14]aneN$_4$). The arrow points to the methyl group of $C(O)CH_3$. The asterisks mark the resonances of the contaminant $(H_2O)L^1CoCH_3^{2+}$, whose ^{13}C spectrum is shown at the top of the figure.

The molecular structure of **1** consists of a six-coordinate cobalt ion surrounded by the four nitrogens of the equatorial macrocyclic ligand, the carbon of the acetyl group, and an oxygen atom of the perchlorate anion. The cobalt atom lies 0.14 Å above the plane of the macrocycle, and three of the four C(11)–Co–N bond angles significantly exceed 90° (Table III). The Co–C bond is "tilted" toward N(2).

In complex **2**, a molecule of H_2O is coordinated to the cobalt trans to the acetyl group. The displacement of cobalt from the N_4 plane is minimal (0.009 Å), and the average C(11)–Co–N bond angle (92.5°) is within 1° of that in the ethyl complex. The Co–OH_2 distance of 2.21 Å in **2** is also comparable to the value for the ethyl complex, 2.20 Å.

The Co–C bond lengths in both acetyl complexes, 1.929 Å (**1**) and 1.915 Å (**2**), are significantly shorter than the Co–C bond in the ethyl complex, 1.99 Å, consistent with the change in hybridization around carbon.

Spectral Data. ^1H and ^{13}C NMR spectra of $(H_2O)L^1CoC(O)CH_3^{2+}$ and its synthetic precursor $(H_2O)L^1CoCH_3^{2+}$ in D_2O are shown in Figures 2 and 3. The methyl resonances in the ^1H spectra appear at 2.91 and 1.48 ppm vs TMS, respectively. As usually happens, the cobalt-bonded carbon is not visible in the ^{13}C spectra, and the only nonmacrocyclic carbon observed is that of the methyl group of $-C(O)CH_3$ at 32.7 ppm. For both complexes, the four resonances grouped together in the 46–52

(11) Melton, J. D.; Espenson, J. H.; Bakac, A. *Inorg. Chem.* **1986**, *25*, 4104.

Table IV. Summary of ^1H and ^{13}C Data for the Methyl and Acetyl Complexes[a]

complex	^1H	^{13}C
$(H_2O)L^1CoCH_3^{2+}$	CH_3: 1.48	N-CH_2: 46.1, 48.8, 50.5, 51.1 C-CH_2: 26.7, 26.9
$(H_2O)L^1CoC(O)CH_3^{2+}$	$C(O)CH_3$: 2.91	$C(O)CH_3$: 32.7 N-CH_2: 46.1, 49.3, 51.0, 51.6 C-CH_2: 26.88, 26.91
$(H_2O)L^2CoCH_3^{2+}$	CH_3: 2.04 (2.13)[b]	

[a] In D_2O; δ vs TMS. L^1 = [14]aneN$_4$; L^2 = Me_6[14]aneN$_4$. [b] Reference 13.

ppm range were assigned[12] to the macrocyclic methylene groups bound to the nitrogens and the two resonances at ~27 ppm to the two unique methylene groups in the six-membered rings of the macrocycle. Both ^1H and ^{13}C spectra of the acetyl complex show some contamination with the starting methyl complex. A summary of all the NMR data is given in Table IV.

The UV–visible data are shown in Table II. The intense transition at ~320 nm is characteristic of the acetyl complexes and has no counterpart in the spectrum of the methyl and other[5,13] alkyl complexes. Above 360 nm, the spectra of the alkyl and acetyl complexes are quite similar, showing two bands in the 450–490- and 360–380-nm ranges. In the acetyl complexes, the latter appears as a weak shoulder on the rising portion of the 320-nm band.

The CO stretch in $[(ClO_4)L^1CoC(O)CH_3](ClO_4)$ appears at 1695 cm^{-1}, in the same general area as for the other acetylcobalt(III) complexes.[14]

Kinetics and Products. The reactions of $(CH_3)_3COOH$ with $LCo(H_2O)_2^{2+}$ (L = L^1, L^2) under argon (eqs 4–6) followed the mixed second-order rate law of eq 7, with k_4 = 52.0 ± 1.5 M^{-1} s^{-1} (L^1) and 11.4 ± 1.4 M^{-1} s^{-1} (L^2).

$$(CH_3)_3COOH + LCo(H_2O)_2^{2+} \rightarrow (H_2O)LCoOH^{2+} + (CH_3)_3CO^{\bullet} + H_2O \quad (4)$$

$$(CH_3)_3CO^{\bullet} \rightarrow CH_3^{\bullet} + (CH_3)_2CO \quad (5)$$

$$CH_3^{\bullet} + LCo(H_2O)_2^{2+} \rightarrow (H_2O)LCoCH_3^{2+} + H_2O \quad (6)$$

$$-d[(CH_3)_3COOH]/dt = k_4[(CH_3)_3COOH][LCo(H_2O)_2^{2+}] \quad (7)$$

After the reduction of all the inorganic Co(III) to the less absorbing 2+ state (see Experimental Section), the UV–visible spectral analysis confirmed the presence of $(H_2O)LCoCH_3^{2+}$ in the amount identical to the initial concentration of $(CH_3)_3COOH$, the rest of the cobalt being present as $LCo(H_2O)_2^{2+}$. The reaction scheme of eqs 4–6 thus fully describes the reaction under the conditions used, and no loss of radicals occurs in radical self-reactions or in a direct reaction between the alkoxyl radicals and $LCo(H_2O)_2^{2+}$ prior to the β scission of eq 5.

The kinetics under CO were identical to those under argon (Figure 4), but the product mixture contained some (H_2O)-$LCoC(O)CH_3^{2+}$ (eq 8), in addition to $(H_2O)LCoCH_3^{2+}$ and

$$CH_3CO^{\bullet} + LCo(H_2O)_2^{2+} \rightarrow (H_2O)LCoC(O)CH_3^{2+} + H_2O \quad (8)$$

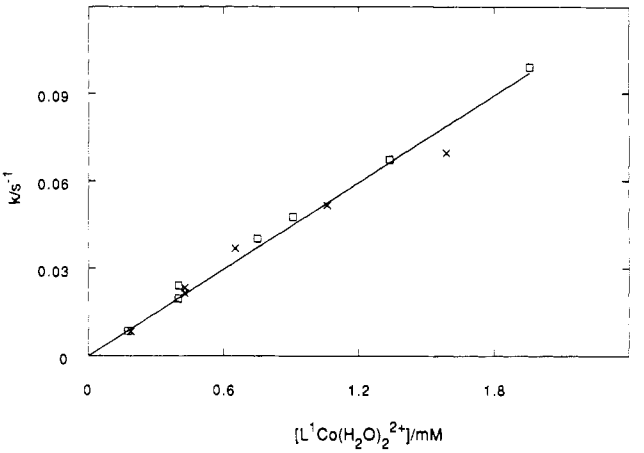

Figure 4. Plot of pseudo-first-order rate constants for the reaction of $(CH_3)_3COOH$ with $L^1Co(H_2O)_2^{2+}$ (L^1 = [14]aneN$_4$) against the concentration of $L^1Co(H_2O)_2^{2+}$ under argon (squares) and CO (crosses).

Table V. Results of the Kinetic Competition Experiments[a]

		$[(H_2O)L^1CoC(O)CH_3^{2+}]_\infty$[b]		
$[t\text{-BuOOH}]_0$	$[L^1Co(H_2O)_2^{2+}]_0$	expt	calc[c]	$[CO]_{av}$
4.0	10.0	0.84	0.80	8.8
1.7	5.0	0.49	0.50	8.7
0.97	4.8	0.28	0.25	8.9
0.78	1.9	0.43	0.44	9.1
0.56	5.2	0.12	0.12	9.1
0.21	0.52	0.15	0.17	9.5
		$[(H_2O)L^2CoC(O)CH_3^{2+}]_\infty$[d]		
$[t\text{-BuOOH}]_0$	$[L^2Co(H_2O)_2^{2+}]_0$	expt	calc[c]	$[CO]_{av}$
1.98	5.16	0.22	0.25	9.2
0.966	2.58	0.21	0.21	9.4
0.607	1.87	0.15	0.15	9.4
0.467	1.25	0.21	0.17	9.4
0.40	3.12	0.052	0.052	9.6

[a] All concentrations in 10^{-4} M; $[H^+]$ = 0.01–0.10 M; 25 °C. L^1 = [14]aneN$_4$; L^2 = Me_6[14]aneN$_4$. [b] Determined spectrophotometrically; l = 5 cm; λ 319 nm (ϵ 1190 M^{-1} cm^{-1}). Correction has been applied for the absorbance of $L^1Co(H_2O)_2^{2+}$ (ϵ 10) and $(H_2O)L^1CoCH_3^{2+}$ (ϵ 100). [c] From eq 9. [d] λ 324 nm (ϵ 834). Correction has been applied for the absorbance of $L^2Co(H_2O)_2^{2+}$ (ϵ 49.1) and $(H_2O)L^2CoCH_3^{2+}$ (ϵ 90.8).

$LCo(H_2O)_2^{2+}$. The yields of the acetylcobalt were quite low in kinetic experiments which utilized a large excess of $LCo(H_2O)_2^{2+}$. The competition for the methyl radicals between CO (eq 3) and $LCo(H_2O)_2^{2+}$ (eq 6) favors reaction 6 owing to the low solubility of CO in aqueous solution[15] and the relatively low value of the rate constant k_3 (see later).

The kinetic competition experiments, designed to determine the value of k_3, therefore utilized only a small excess of $LCo(H_2O)_2^{2+}$ over the stoichiometric 2:1 ratio. The results for both complexes are shown in Table V. The data were fitted[4] to eq 9 and gave k_3 = (2.3 ± 0.1) × 10^6 M^{-1} s^{-1} (L = L^1) and (1.8 ± 0.1) × 10^6 (L = L^2), yielding an average value of k_3 = (2.0 ± 0.3) × 10^6 M^{-1} s^{-1}.

$$[(H_2O)LCoC(O)CH_3^{2+}]_\infty = -\left(\frac{k_3[CO]_{av}}{2k_6}\right) \ln\left(1 - \frac{2[(CH_3)_3COOH]_0}{[LCo(H_2O)_2^{2+}]_0 + (k_3[CO]_{av}/k_6)}\right) \quad (9)$$

Laser flash photolysis of $(H_2O)L^1CoC(O)CH_3^{2+}$ in the presence of 0.07–0.30 mM $C(NO_2)_4$ (hereafter TNM) resulted in a *single-*

(12) Shoulders, B.; Welch, S. C. *J. Chem. Educ.* **1987**, *64*, 915.
(13) Roche, T. S.; Endicott, J. F. *J. Am. Chem. Soc.* **1972**, *94*, 8622.
(14) (a) Floriani, C.; Puppis, M.; Calderazzo, F. *J. Organomet. Chem.* **1968**, *12*, 209. (b) Costa, G.; Mestroni, G. *Tetrahedron Lett.* **1967**, 1783. (c) Bigoto, A.; Costa, G.; Mestroni, G.; Pellizer, G.; Puxeddu, A.; Reisenhofer, E.; Stefani, L.; Tauzher, G. *Inorg. Chim. Acta Rev.* **1970**, *4*, 41.
(15) *Solubility Data Series, Carbon Monoxide*; Cargill, R. W., Ed.; Pergamon Press; p 2. It was assumed that submillimolar concentrations of $LCo(H_2O)_2^{2+}$ and *t*-BuOOH had no effect on the solubility of CO in H_2O.

stage, first-order absorbance increase at 350 nm, a maximum for the nitroform anion, $C(NO_2)_3^-$. The measured rate constants all lie in the range $(1.7–2.9) \times 10^4$ s^{-1}. These results show that photolysis produces acetyl radicals, $CH_3C^{\bullet}O$, and not the hydrated form, $CH_3C^{\bullet}(OH)_2$. The reaction of the hydrated form with TNM is rapid ($k = 2.8 \times 10^9$ M^{-1} s^{-1}),[16] whereas $CH_3C^{\bullet}O$ has been reported to react only indirectly after hydration to $CH_3C^{\bullet}(OH)_2$; $k_{hydr} \sim 2 \times 10^4$ s^{-1}. The single-stage kinetic traces in the present work obviously rule out the immediate presence of both forms of the radical. The rate constants measured are in the correct range for k_{hydr} but are much too small for the direct reaction of TNM with $CH_3C^{\bullet}(OH)_2$.

However, the rate constants show an unexpected trend with [TNM]. A plot of k_{obs} vs [TNM] is linear with an intercept of 1.5×10^4 s^{-1} and a slope of 4.5×10^7 M^{-1} s^{-1}. At an average radical concentration of ~ 2 μM, a contribution from the radical self-reaction is unlikely[17] to exceed 4×10^3 s^{-1}, leaving $k_{hydr} \sim 1.1 \times 10^4$ s^{-1}. The slope of the line, $k_{TNM} = 4.5 \times 10^7$ M^{-1} s^{-1}, represents the rate constant for the direct reaction of $CH_3C^{\bullet}O$ with TNM. This reaction is much slower than that of the hydrated radical, but not completely negligible as previously thought.[16] Careful analysis of the data in ref 16 shows that in that work there was also a slight trend in k_{obs} with [TNM], but this was ignored[16] in the analysis, presumably because the range of [TNM] used was considered too narrow to obtain a reliable value of the slope. Our analysis of the data in ref 16 yields $k_{hydr} \sim 1.7 \times 10^4$ s^{-1} and $k_{TNM} \sim 4 \times 10^7$ M^{-1} s^{-1}. Our results are in acceptable agreement with these values.

The laser flash photolysis of $(H_2O)L^1CoC(O)CH_3^{2+}$ (λ_{exc} 355 nm) in the presence of 2.1–10.6 mM Cr^{2+} resulted in a first-order absorbance increase at 320 nm. A plot of k_{obs} against the concentration of Cr^{2+} is linear with a negligible intercept and a slope of $(3.1 \pm 0.2) \times 10^8$ M^{-1} s^{-1}, in both argon- and CO-saturated solutions. This value is comparable to those for the reactions of Cr^{2+} with other C-centered radicals,[18] and we presume $(H_2O)_5CrC(O)CH_3^{2+}$ results.

Discussion

Kinetics. The rate constant k_3 for the capture of $CH_3^{\bullet}$ by CO in aqueous solution determined in this work is 2.0×10^6 M^{-1} s^{-1}, some 300 times larger than the reported gas-phase value.[1] In aqueous solution, reaction 3 is thus a feasible *and practical* route to the acetyl radicals at atmospheric CO pressures, as demonstrated by the quantitative photochemical conversion of $(H_2O)LCoCH_3^{2+}$ to $(H_2O)LCoC(O)CH_3^{2+}$. A route to other such photochemical CO insertions thus appears to be wide open. This is true not only for the conversion of methyl to acetyl complexes but also for the conversion of the higher analogues. For example, qualitative experiments with $(H_2O)L^1CoC_2H_5^{2+}$ yielded solutions with an intense absorption maximum at 316 nm, suggestive of the propionyl complex.

Obviously, the success of the acyl-forming reaction (1) depends on the kinetics of the forward step and the equilibrium constant K_1. The values of K_1 are not available in solution, but the rate constants for decarbonylation of acyl radicals, k_{-1}, cover over 15 orders of magnitude[19] and correlate strongly with the stability of the radicals R$^{\bullet}$. If one assumes that k_1 does not change greatly throughout the series, then the values of K_1 also span ~ 15 orders of magnitude. On the basis of the actual values[19] of k_{-1}, reaction 1 is not expected to be useful synthetically for radicals other than phenyl and primary alkyls.

The large increase in k_3 as the reaction is transferred from the gas phase into aqueous solution probably reflects the stabilization of the polar acetyl radical by dipolar interactions with the solvent.

The determination of k_3 in this work is based on the assumptions that $LCo(H_2O)_2^{2+}$ complexes react with $(CH_3)_3COOH$ according to eqs 3–6 and 8 and that the competition between reactions 3 and 6 determines the yield of the acetylcobalt complex. There is little doubt that in the absence of CO the reaction indeed proceeds as described in eqs 4–6. This has been well established by the formation of the aqua and methyl complexes in a 1:1 ratio, quantitative yields of acetone, and correct kinetic dependences. In the presence of CO, reaction 3 will clearly become part of the picture, but this does not automatically make it the only source of acetylcobalt, or even a major one.

Another mechanism that might account for the formation of $(H_2O)LCoC(O)CH_3^{2+}$ is described in reactions 10 and 11,

$$LCo(H_2O)_2^{2+} + CO \rightleftarrows (H_2O)LCoCO^{2+} + H_2O \quad (10)$$

$$(H_2O)LCoCO^{2+} + CH_3^{\bullet} \rightarrow (H_2O)LCoC(O)CH_3^{2+} \quad (11)$$

according to which the carbonylcobalt complex is formed first. Subsequent reaction with $CH_3^{\bullet}$ then yields the observed product. We discard this mechanism both on chemical grounds and from the results of chemical competition experiments. First, it is unlikely that significant amounts of the carbonyl complex exist in solution, given that CO has no effect on spectral or kinetic properties of $LCo(H_2O)_2^{2+}$. For example, the reaction with $(CH_3)_3COOH$ takes place with an identical rate constant under argon and CO atmospheres.

If, on the other hand, only minute quantities of the carbonyl complex are present, then the rate constant for its reaction with $CH_3^{\bullet}$ has to be unreasonably large (>10^9 M^{-1} s^{-1}) to compete successfully with the irreversible capture of $CH_3^{\bullet}$ by the predominant cobalt(II) species, $LCo(H_2O)_2^{2+}$. The latter reaction, eq 6, has a rate constant[18a] of 1.6×10^7 M^{-1} s^{-1} for L^1 and 4.2×10^7 for L^2.

The most convincing argument in favor of the mechanism in eqs 3–6 and 8 is the good fit of experimental data to eq 9. Specifically, the yield of the acetylcobalt decreases with an increase in [$LCo(H_2O)_2^{2+}$] (Table V), as expected for a competition between reactions 3 and 6. In the mechanism of eqs 10 and 11, the dependence on [$LCo(H_2O)_2^{2+}$] disappears, because a change in this concentration affects equally the yields of methyl- and acetylcobalt complexes.

Solid-State Structure of the Acetyl Complexes. In both **1** and **2**, the macrocyclic ligand adopts the thermodynamically stable *R,R,S,S* configuration at nitrogens. Both complexes are hexacoordinated with either the perchlorate (**1**) or H_2O (**2**) occupying the sixth coordination position. The acetyl ligand is free to rotate about the Co–C bond. A comparison of the N–Co–C–O torsion angles shows that the acetyl group is rotated by 93° between **1** and **2**.

Solution Structure of the Acetyl Complexes. The laser flash photolysis of $(H_2O)LCoC(O)CH_3^{2+}$ represents a convenient route to acetyl radicals, as demonstrated by the kinetic study of the reaction with Cr^{2+}. The formation of $CH_3C^{\bullet}O$ as the initial photolytic product establishes unequivocally that the solution form of the complex is $(H_2O)LCoC(O)CH_3^{2+}$ and not the hydrated species $(H_2O)LCoC(OH)_2CH_3^{2+}$. This explains the stability of the complex even in the absence of added $LCo(H_2O)_2^{2+}$. The hydrated form, in effect an α,α-dihydroxyalkyl complex, would be expected to homolyze rapidly. Some other acetylcobalt

(16) Schuchmann, M. N.; Von Sonntag, C. *J. Am. Chem. Soc.* **1988**, *110*, 5698.
(17) A typical rate constant for radical self-reactions is $2k \sim 2 \times 10^9$ M^{-1} s^{-1} (Ross, A. B.; Neta, P. *Rate Constants for Reactions of Aliphatic Carbon-Centered Radicals in Aqueous Solution*; NSRDS-NBS 70; National Bureau of Standards: Washington, DC, 1982.
(18) (a) Bakac, A.; Espenson, J. H. *Inorg. Chem.* **1989**, *28*, 3901. (b) Bakac, A.; Espenson, J. H. *Inorg. Chem.* **1989**, *28*, 4319. (c) Cohen, H.; Meyerstein, D. *Inorg. Chem.* **1974**, *13*, 2434.
(19) Fischer, H.; Paul, H. *Acc. Chem. Res.* **1987**, *20*, 200.

compounds have been used previously[20] as photochemical sources of acetyl radicals in nonaqueous solutions.

Acknowledgment. We are indebted to Mr. Wen-Jang Chen for his help with the NMR measurements and to Drs. Siquan Luo and John McClelland for the use of their FTIR spectrometer and for their help in obtaining the IR spectra. We also thank Dr. R. Angelici and Dr. J. Corbett for useful discussions. This work was supported by the Office of Basic Energy Sciences, Chemical Sciences Division, U.S. Department of Energy, under Contract W-7405-Eng-82.

(20) Coveney, D. J.; Patel, V. F.; Pattenden, G. *Tetrahedron Lett.* **1987**, *28*, 5949.

Supplementary Material Available: Listings of atomic positional parameters, general anisotropic displacement parameter expressions, bond lengths and angles, and root-mean-square amplitudes of anisotropic displacement and unit cell packing diagrams (13 pages). Ordering information is given on any current masthead page.